Advanced Node Formulations in TLM—The Adaptable Symmetrical Condensed Node

Vladica Trenkic, *Member, IEEE*, Christos Christopoulos, *Member, IEEE*, and Trevor M. Benson, *Member, IEEE*

***Abstract*— The paper describes the development of a class of adaptable symmetrical condensed (ASCN) transmission-line modeling (TLM) nodes. The parameters and numerical properties of the ASCN are expressed in terms of arbitrary weighting functions which can be selected in a manner that minimizes dispersion and improves accuracy. It is shown that this approach is effective and can be used to optimize nodal properties according to problem requirements.**

I. Introduction

THE PROCESS of discretization in space, inherent to all numerical solution schemes, introduces propagation errors in the transmission-line modeling (TLM) method. Dispersion analysis of three-dimensional (3-D) TLM schemes, modeling free space on a cubic node mesh, shows that the symmetrical condensed node (SCN) exhibits substantially smaller propagation error than the expanded node (EN) and an equivalent Yee's finite-difference time-domain (FDTD) scheme [1]. Additional propagation errors are, however, introduced when modeling nonuniform materials and/or using noncubic nodes and this can eliminate the primary advantage of the SCN over the EN [2]–[5]. These errors decrease as space resolution increases, but there are practical limitations, brought about by run-time and storage requirements, to the extent that accuracy can be improved in this way. Hence, other approaches are explored here to develop more accurate schemes based on the SCN.

Local deviation in material properties and changes of cell aspect ratio are described in the TLM SCN by adding stubs and/or modifying the link line impedances [6]–[9]. Based on the TLM constitutive equations [10], an infinite set of SCN-based schemes can be developed. All these schemes can be unified through the formulation of a general SCN (GSCN) [11], [12]. Applying additional constraints to the GSCN, the traditional stub-loaded SCN [6], hybrid SCN (HSCN) [7], symmetrical super-condensed node (SSCN) [8] and matched SCN (MSCN) [9], as well as other new, hitherto unexplored, schemes, can be derived.

The dispersion analysis of the various SCN-based TLM schemes suggests that stub-loading and changing of the link-line impedances make opposing contributions to the dispersion [4], [9], [13]. In this paper, we exploit these effects to develop a class of novel nodes, with a mix of links and stubs which secure advantageous dispersion properties. As these nodes can be customized (adapted) through arbitrary weighting functions, they are referred to as the adaptable SCN (ASCN).

In this paper, the complete theoretical development of the ASCN for a uniform mesh is presented first, including the dispersion analysis and the derivation of possible optimizing weighting functions. Then, the parameters and numerical properties of the noncubic ASCN for a graded mesh are investigated and, finally, the theoretical results are validated by simulations of partially filled waveguides.

Manuscript received March 27, 1996. This work was supported in part by the Engineering and Physical Sciences Research Council, U.K.

The authors are with the Department of Electrical and Electronic Engineering, University of Nottingham, Nottingham NG72RD U.K.

Publisher Item Identifier S 0018-9480(96)08524-9.

II. Adaptable Node for the Uniform Mesh

The parameters of a GSCN must satisfy the TLM constitutive relations, which can be written in a compact form as [9]

$$Y_{ik} + Y_{jk} + \frac{Y_{ok}}{2} = \varepsilon \frac{\Delta i \Delta j}{\Delta k \Delta t} \tag{1}$$

$$Z_{ij} + Z_{ji} + \frac{Z_{sk}}{2} = \mu \frac{\Delta i \Delta j}{\Delta k \Delta t} \tag{2}$$

where $i, j, k \in \{x, y, z\}$ and $i \neq j, k$ with $\varepsilon = \varepsilon_0 \varepsilon_r$ and $\mu = \mu_0 \mu_r$. The characteristic impedance and admittance of i-directed, j-polarized link lines are denoted by Z_{ij} and Y_{ij}, respectively. The admittance of an open-circuit stub and the impedance of a short-circuit stub, coupling with the field components in the k direction, are denoted by Y_{ok} and Z_{sk}, respectively.

In the case of the general node for a uniform mesh of node spacings $\Delta x = \Delta y = \Delta z = \Delta l$, the TLM constitutive relations (1)–(2) reduce to

$$Y_n + Y_p + \frac{Y_o}{2} = \varepsilon \frac{\Delta l}{\Delta t} \tag{3}$$

$$Z_n + Z_p + \frac{Z_s}{2} = \mu \frac{\Delta l}{\Delta t} \tag{4}$$

where

$$Z_p = 1/Y_p = Z_{xy} = Z_{yz} = Z_{zx}$$
$$Z_n = 1/Y_n = Z_{yx} = Z_{zy} = Z_{xz}$$
$$Y_o = Y_{ox} = Y_{oy} = Y_{oz}$$
$$Z_s = Z_{sx} = Z_{sy} = Z_{sz}.$$

If we specify that the link lines will model a proportion of the medium parameters denoted by $(w_\varepsilon \varepsilon, w_\mu \mu)$, where w_ε and w_μ are arbitrary dimensionless weights, it follows that

$$Y_n + Y_p = w_\varepsilon \varepsilon \frac{\Delta l}{\Delta t} \tag{5}$$

$$Z_n + Z_p = w_\mu \mu \frac{\Delta l}{\Delta t}. \tag{6}$$

Relating the velocity of pulses on the link lines to the wave velocity in free-space (background medium) as [14]

$$\frac{\Delta l}{\Delta t} = \frac{2}{\sqrt{\varepsilon_0 \mu_0}} \tag{7}$$

and solving (5) and (6), the link-line impedances are obtained as

$$Z_n = Z_1 A \quad Z_p = Z_1 / A \tag{8}$$

where

$$Z_1 = Z\sqrt{\frac{w_\mu}{w_\varepsilon}} \tag{9}$$

$$A = A_{1,2} = \sqrt{w_\varepsilon w_\mu \mu_r \varepsilon_r} \pm \sqrt{w_\varepsilon w_\mu \mu_r \varepsilon_r - 1}. \tag{10}$$

The parameters of the stubs, used to model the remaining proportion of the medium properties, can be obtained by inserting (5)–(6) into (3)–(4) and making use of (7), as

$$Y_o = 4Y\sqrt{\varepsilon_r \mu_r}(1 - w_\varepsilon) \tag{11}$$

$$Z_s = 4Z\sqrt{\varepsilon_r \mu_r}(1 - w_\mu) \tag{12}$$

where $Z = 1/Y = \sqrt{\mu/\varepsilon}$.

The parameters of the GSCN for a uniform mesh are therefore defined by (8)–(12) in terms of the arbitrary weights w_ε and w_μ. For example, the stub-loaded SCN is defined by (8)–(12) if $w_\varepsilon = 1/\varepsilon_r$ and $w_\mu = 1/\mu_r$. Similarly, selecting $w_\varepsilon = 1/(\varepsilon_r \mu_r)$ and $w_\mu = 1$, the HSCN is formulated. In the case of the SSCN, the requirements are $w_\varepsilon = w_\mu = 1$, while for the MSCN we need $w_\varepsilon = w_\mu = 1/\sqrt{\varepsilon_r \mu_r}$.

The dispersion behavior of the available condensed nodes can be interpreted through parameters w_ε and w_μ. For example, dispersion in the stub-loaded SCN is dependent on the ratio ε_r/μ_r for $\varepsilon_r \mu_r = \text{const}$ [2]–[4], which is a direct result of w_ε and w_μ not being functions of the product $\varepsilon_r \mu_r$. Similarly, two solutions to the dispersion relation, corresponding to different field polarizations, are experienced in the stub-loaded SCN and the HSCN [2], [4], [5], which is a consequence of selecting $w_\varepsilon \neq w_\mu$. As this behavior is at variance with Maxwell's equations, we avoid it in the development of the ASCN, presented here, by choosing $w_\varepsilon = w_\mu = w$, where w is a function of the product $\varepsilon_r \mu_r$. The parameters of the ASCN, normalized to the impedance and admittance of the modeled medium, Z and Y, can be obtained, after inserting $w_\varepsilon = w_\mu = w$ in (8)–(12), as

$$\hat{Z}_n = A \quad \hat{Z}_p = 1/A \tag{13}$$

$$\hat{Y}_o = \hat{Z}_s = 4\sqrt{\varepsilon_r \mu_r}(1 - w) \tag{14}$$

where

$$A = A_{1,2} = w\sqrt{\mu_r \varepsilon_r} \pm \sqrt{w^2 \mu_r \varepsilon_r - 1}. \tag{15}$$

Note that two solutions exist for A. It can be readily proved that $A_1 = 1/A_2$. Hence, choosing different signs in (15) will swap values of Z_n and Z_p. As shown later, both solutions are physical.

In order to satisfy the requirement that the link and stub parameters are real and nonnegative numbers, it follows from (14) that $w \leq 1$ and from (15) that $w \geq 1/\sqrt{\varepsilon_r \mu_r}$. The SSCN and the MSCN can be considered as special, limiting cases of the adaptable node with $w = 1$ and $w = 1/\sqrt{\varepsilon_r \mu_r}$, respectively.

Using the definition of scattering in the general condensed node [12], the scattering properties of the ASCN can be readily obtained. Following the approach described in [3], the dispersion relation of the ASCN can be obtained from the general dispersion relation [1] in an implicit polynomial form as

$$\cos 4\theta + B_1 \cos 3\theta + B_2 \cos 2\theta + B_3 \cos\theta + \frac{B_4}{2} = 0 \tag{16}$$

where $\theta = 2\pi f \Delta t$ and

$$\begin{aligned}
B_1 &= 2s_1(1 - w) + 4 \\
B_2 &= w^2u^2(2s_1 + s_2) + w^2(3s_2 - 2s_1) - 4w(s_1 + 2s_2) \\
&\quad + 4(s_1 + s_2 + 1) \\
B_3 &= -2w^3u^2(3s_3 + 2s_2) - 2w^3(s_3 - 2s_2) \\
&\quad + 2w^2u^2(3s_3 + 4s_2 + 4s_1) + 2w^2(9s_3 - 4s_2 - 4s_1) \\
&\quad - 2w(12s_3 - s_1) + 2(4s_3 - s_1 - 2) \\
B_4 &= -4w^3u^2(3s_3 + 2s_2) + 4w^3(7s_3 + 2s_2) \\
&\quad + 2w^2u^2(6s_3 + 7s_2 + 6s_1) - 2w^2(30s_3 + 11s_2 + 6s_1) \\
&\quad + 8w(6s_3 + 2s_2 + s_1) - 2(8s_3 + 4s_2 + 4s_1 + 5)
\end{aligned}$$

with

$$\begin{aligned}
u &= \sqrt{1 - \frac{1}{w^2 \varepsilon_r \mu_r}} \\
s_1 &= c_x + c_y + c_z \\
s_2 &= c_x c_y + c_y c_z + c_z c_x \\
s_3 &= c_x c_y c_z
\end{aligned}$$

and $c_x = \cos(k_x \Delta l) - 1$, $c_y = \cos(k_y \Delta l) - 1$ and $c_z = \cos(k_z \Delta l) - 1$, where k_x, k_y, and k_z are Cartesian components of the propagation vector. Note that the dispersion relation is obtained in terms of the weighting function w and that it is independent of the selection of the $+$ or $-$ sign appearing in (15).

Since the SSCN and the MSCN can be considered as the two limiting cases of the ASCN, we first examine their dispersion behavior. Note that the SSCN does not use stubs at all and therefore all excess material parameters are modeled solely through the variation of the link-line impedances. In contrast to this, in the MSCN the characteristic impedance of link lines is the same and matches the intrinsic impedance of the medium, hence all excess material parameters are modeled exclusively through the stubs [9]. From the dispersion analysis it can be seen that these two approaches in modeling the variation in material parameters have opposing effects on propagation errors. This is illustrated in Fig. 1 by plotting the relative deviation in the propagation vector for a benchmark discretization of ten nodes per wavelength, referred to as the normalized propagation error [4]. The error is presented for three principal propagation directions: along an axis (e.g., $[1, 0, 0]$), a diagonal in a coordinate plane (e.g., $[1, 1, 0]$) and the space diagonal ($[1, 1, 1]$).

The weighting function for the ASCN can have any value limited by $w = 1/\sqrt{\varepsilon_r \mu_r}$ (MSCN) and $w = 1$ (SSCN). In

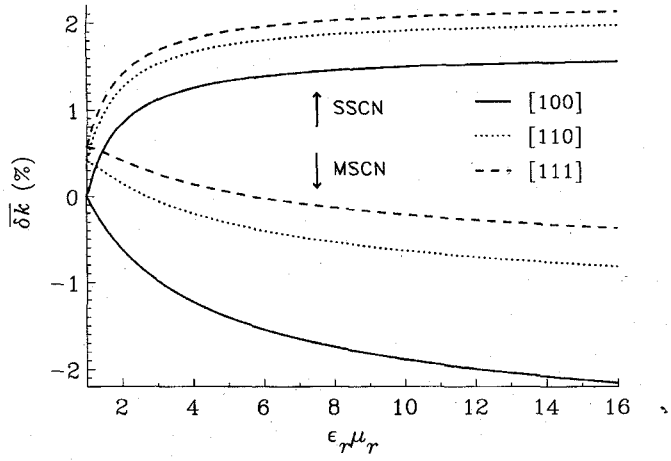

Fig. 1. Percentage propagation error in the MSCN and the SSCN for $\Delta l/\lambda = 0.1$.

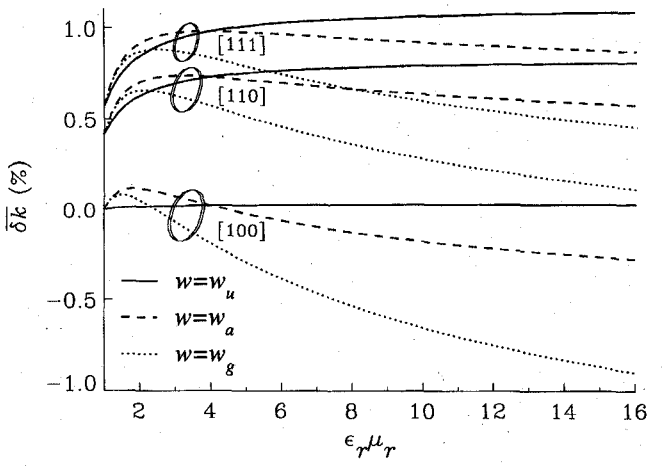

Fig. 2. Percentage propagation error in the ASCN for $\Delta l/\lambda = 0.1$ using w_u, w_a, and w_g.

order to compensate errors occurring in the MSCN and SSCN, the weighting function w of the ASCN could be chosen as a suitable mean of these limits, for example, the arithmetic and geometric means, given by

$$w_a = \frac{\sqrt{\varepsilon_r\mu_r}+1}{2\sqrt{\varepsilon_r\mu_r}} \quad \text{and} \quad w_g = \frac{1}{\sqrt[4]{\varepsilon_r\mu_r}} \tag{17}$$

respectively. The weighting function w can be also selected according to problem requirements, for example, demanding minimal propagation error for the axial direction. By inserting $k_x\Delta l = 2\theta\sqrt{\varepsilon_r\mu_r}$ and $k_y = k_z = 0$ in (16) and solving for w, we obtain

$$w = \frac{\cos(\theta)+\cos(2\theta\sqrt{\varepsilon_r\mu_r})}{\cos(2\theta\sqrt{\varepsilon_r\mu_r})-1} + \frac{1}{2\varepsilon_r\mu_r(1-\cos(\theta))}. \tag{18}$$

It can be seen from (18) that the solution for w is, of course, dependent on $\theta = 2\pi f\Delta t$, i.e., on the frequency. Since TLM operates with several nodes per wavelength, corresponding to a relatively low frequency, the limit of (18) can be sought when $\theta \to 0$, leading to a surprisingly simple result for w given by

$$w = w_u = \frac{1+2\varepsilon_r\mu_r}{3\varepsilon_r\mu_r}. \tag{19}$$

Using the three functional forms of w described by (17) and (19), the propagation errors of the ASCN for three principal propagation directions are plotted in Fig. 2. A comparison between the propagation errors of the ASCN, plotted in Fig. 2, and those of the SSCN and the MSCN plotted in Fig. 1, clearly demonstrates that the error in the ASCN, for any of the weighting functions used, is indeed contained between the errors of the MSCN and the SSCN. A direct result of this is that the error range in the ASCN with $w = w_a$ and particularly with $w = w_u$ is significantly smaller than in the SSCN and MSCN.

Fig. 3 shows the percentage propagation error for the ASCN with $w = w_u$ for different values of $\varepsilon_r\mu_r$ and for propagation along the coordinate plane $y = 0$ and the diagonal plane $x = y$. The error is plotted versus the angle φ formed by the propagation vector and the z-axis. In this case, propagation along directions $[m, 0, n]$ (coordinate plane), and $[m, m, n]$ (diagonal plane) can be studied. Some of these directions are indicated in the figure. It can be seen from Fig. 3 that errors in the ASCN with $w = w_u$ extend only in the positive direction (unilateral dispersion) and increase slowly with an increase in $\varepsilon_r\mu_r$.

Fig. 4 compares the propagation errors for the ASCN ($w = w_u$) with those obtained using the MSCN and the SSCN, for propagation along the diagonal plane $x = y$. It is evident from this plot that a substantial reduction in propagation errors is obtained with the ASCN, allowing for a more accurate modeling of nonuniform problems in TLM than was allowed by the previous nodes.

III. Adaptable Node for a Graded Mesh

Parameters of the noncubic ASCN used in a graded mesh can be obtained from the general TLM relations (1)–(2) using a similar procedure as for the cubic ASCN. The proportion of the medium properties modeled by the link lines alone can be written for a graded node as

$$Y_{ik} + Y_{jk} = w_{\varepsilon k}\varepsilon\frac{\Delta i\Delta j}{\Delta k\Delta t} \tag{20}$$

$$Z_{ij} + Z_{ji} = w_{\mu k}\mu\frac{\Delta i\Delta j}{\Delta k\Delta t}. \tag{21}$$

Using a similar reasoning as before, to avoid polarization-dependent dispersion solutions, we choose $w_{\varepsilon k} = w_{\mu k} = w_k$. With this condition, the system of six equations, (20)–(21), formed by using all possible combinations of $i, j, k \in \{x, y, z\}$, can be solved in a similar manner as the system of equations describing the parameters of the graded SSCN [8]. Introducing

$$\Delta i' = \Delta i\sqrt{w_j w_k} \tag{22}$$

for all combinations of $i, j, k \in \{x, y, z\}$ into (20)–(21), the normalized admittances of the link lines are obtained as

$$\hat{Y}_{ij} = \sqrt{\varepsilon\mu}\frac{\Delta i'\Delta k'\hat{C}_{ij}}{\Delta t\Delta j'}. \tag{23}$$

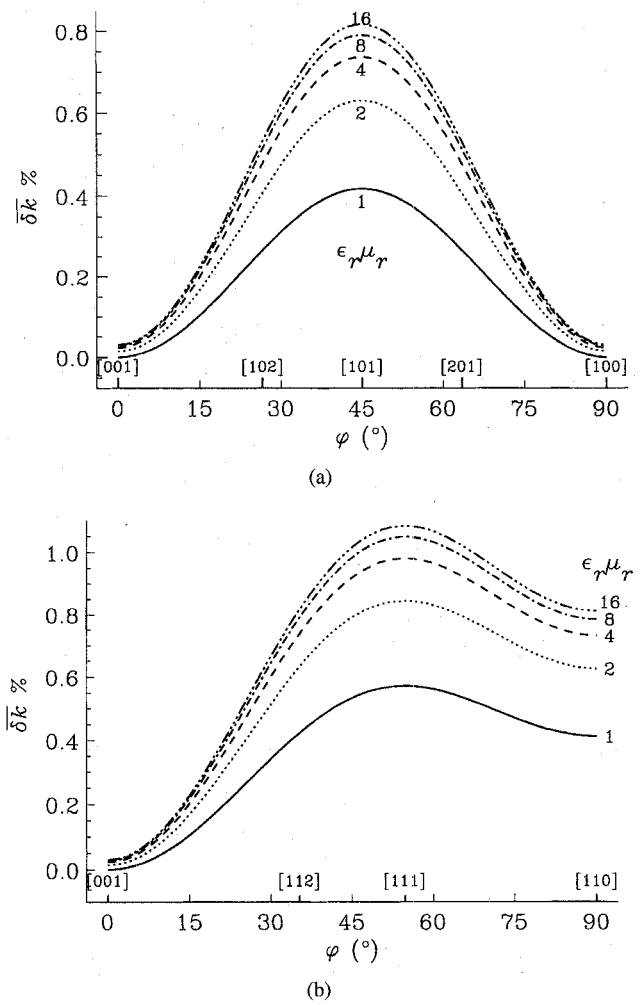

Fig. 3. Percentage propagation error in the ASCN ($w = w_u$) for propagation along (a) coordinate plane $y = 0$ and (b) diagonal plane $x = y$ ($\Delta l/\lambda = 0.1$).

For $(i,j,k) \in \{(x,y,z),(y,z,x),(z,x,y)\}$, the normalized capacitance $\hat{C}_{ij}$ [8] is

$$\hat{C}_{ij} = \frac{2(\Delta j')^2(\Delta k')^2 + B}{2(\Delta i')^2(\Delta k')^2[\varepsilon\mu(\Delta j'/\Delta t)^2 - 1]} \tag{24}$$

with

$$B_{1,2} = A \pm \sqrt{A^2 - \frac{(2\Delta x'\Delta y'\Delta z'\Delta t)^2}{\varepsilon\mu}} \tag{25}$$

and

$$A = (\Delta x'\Delta y'\Delta z')^2\left(\frac{\varepsilon\mu}{(\Delta t)^2} - \frac{1}{(\Delta x')^2} - \frac{1}{(\Delta y')^2} - \frac{1}{(\Delta z')^2}\right). \tag{26}$$

The remaining three normalized capacitances are obtained as

$$\hat{C}_{kj} = 1 - \hat{C}_{ij}. \tag{27}$$

Following the procedure outlined for the SSCN in [8], the maximum time step is determined from (25) as

$$\Delta t_{\max} = \frac{\varepsilon\mu H}{2\cos\left[\frac{1}{3}\arccos(H^3/G)\right]} \tag{28}$$

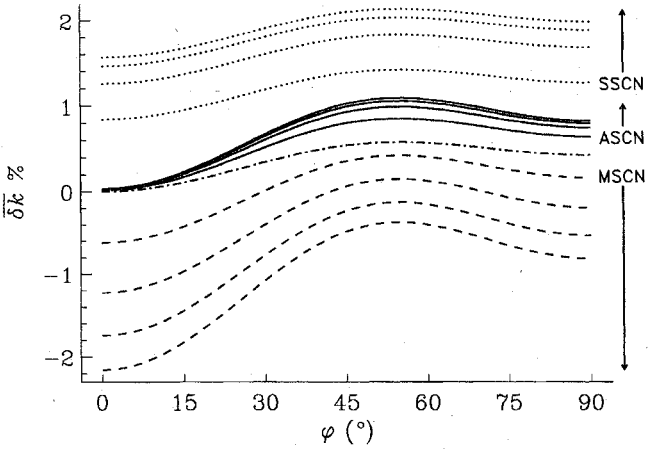

Fig. 4. Comparison of propagation errors in the ASCN with $w = w_u$ (solid lines), the SSCN (dotted lines) and the MSCN (broken lines) for $\Delta l/\lambda = 0.1$ and $\varepsilon_r\mu_r \in \{2,4,8,16\}$(direction of the increase in $\varepsilon_r\mu_r$ is denoted by arrows).

where

$$H = \sqrt{\frac{3}{(\Delta x')^{-2} + (\Delta y')^{-2} + (\Delta z')^{-2}}} \quad G = \Delta x'\Delta y'\Delta z'.$$

Finally, the parameters of the stubs, used to model the remaining proportion of the medium properties, can be obtained by inserting (20)–(21) into (3)–(4), as

$$\hat{Y}_{ok} = \hat{Z}_{sk} = 2\sqrt{\varepsilon\mu}\,\frac{\Delta i\Delta j}{\Delta k\Delta t}(1 - w_k). \tag{29}$$

The presence of three weighting functions in the definition of the graded ASCN offers great flexibility for optimizing nodal properties. Weighting functions w_x, w_y, and w_z can be selected either independently or selected to be equal, $w_x = w_y = w_z = w$. As an example, we give the analysis of the latter case.

As in the case of cubic nodes, the graded ASCN simplifies to the graded SSCN when $w = 1$. It is known that the SSCN exhibits the lowest numerical dispersion when operating on its maximum time step [15]. This dispersion is generally lower than that for the other available schemes, e.g., the HSCN [13], but it increases rapidly when the SSCN operates on a time step lower than the maximum one. Since the SSCN scheme provides the highest possible time step for a given node aspect ratio [8], the weighting function of the ASCN could sensibly be selected in a manner to give $w = 1$ when $\Delta t = \Delta t_{\max}$. In the SSCN, as a limiting case of the ASCN ($w = 1$), all deviations in the wave velocity are modeled through the variation of link-line impedances. Another limiting case is when the deviations in velocity are modeled exclusively through the stubs, which is obtained by choosing $w = w_{\min} = \Delta t/\Delta t_{\max}$. In this case, the ASCN behaves in a similar manner as the MSCN—in fact, for a cubic node mesh it follows that

$$\frac{\Delta t}{\Delta t_{\max}} = \frac{1}{\sqrt{\varepsilon_r\mu_r}} \tag{30}$$

and the ASCN with $w_{\min}$ reduces to the MSCN. As an example, Fig. 5 shows that by decreasing the time step, the initial propagation error is shifted in the opposite directions

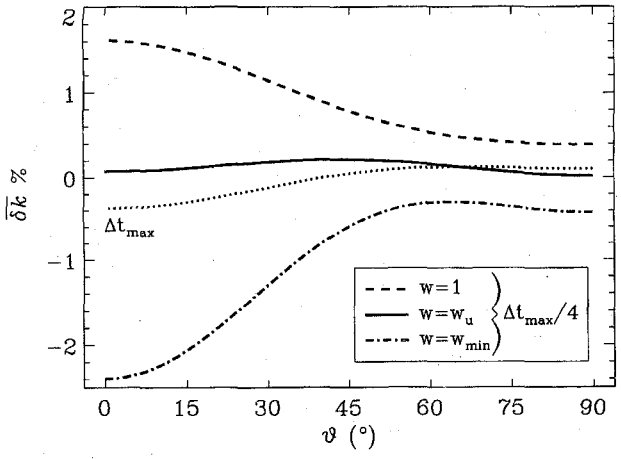

Fig. 5. Percentage propagation error in graded ASCN ($\Delta x = 2\Delta y = \Delta z$) for discretization of $\Delta x/\lambda = 0.1$ and propagation in coordinate plane $z = 0$ (ϑ is angle formed by the propagation vector and the x-axis).

when using the two limiting choices of w, that is, $w = 1$ and $w = w_{\min}$. Hence, to compensate errors, the optimization of the graded ASCN can be achieved by obtaining weighting functions as an average of $\Delta t/\Delta t_{\max}$ and unity.

Making use of (30), the weighting functions described by (17) and (19) for a cubic ASCN can be rewritten in terms of $\Delta t/\Delta t_{\max}$, and used for the graded ASCN. For example, the propagation error for a graded ASCN with $w = w_u$ is shown in Fig. 5. It is evident from the plot that the propagation error with $w = w_u$ is constrained by the two extreme cases and is very low.

IV. Numerical Examples

In order to confirm the predicted numerical properties of the adaptable nodes explored above, we modeled a partially filled canonical waveguide ($a = 2.286$ cm, $b = 1.016$ cm, $h = b/3$, $\varepsilon_r = 2.56$), depicted in Fig. 6, using a uniform TLM mesh with node spacing $\Delta l = b/12$. TLM simulations were performed using adaptable nodes with weighting functions $w = w_u$ (denoted by ASCN), $w = 1$ (SSCN), $w = 1/\sqrt{\varepsilon_r \mu_r}$ (MSCN), as well as using the HSCN (which in this case equals the traditional stub-loaded SCN). Two sets of results were obtained with the SSCN and the ASCN by swapping values of Z_n and Z_p. The analytical cutoff frequencies of the hybrid TE^y modes were obtained using the transverse resonance method [16]. A summary of the cutoff frequencies obtained for the first four hybrid TE^y_{m1} modes is presented in Table I.

As expected, all results converge to the analytical solutions and results obtained with the ASCN are always between the results obtained with the SSCN and the MSCN. In order to facilitate comparison of these results with the predictions based on the dispersion analysis, we calculated propagation errors normalized to 10 nodes per wavelength in the dielectric, by using the formula [3]

$$\overline{\delta k} = \frac{(f_0 - f)}{f}\left(\frac{0.1}{\Delta l/\lambda}\right)^2 = \frac{(f_0 - f)}{f}\left(\frac{0.1c}{\Delta l f_0 \sqrt{\varepsilon_r}}\right)^2 \quad (31)$$

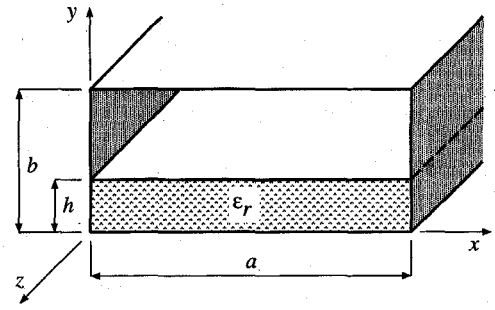

Fig. 6. Partially loaded rectangular waveguide.

TABLE I
Cutoff Frequencies in GHz

	TE^y_{01}	TE^y_{11}	TE^y_{21}	TE^y_{31}
Analytical	12.612	13.734	16.544	20.120
SSCN_1	12.597	13.692	16.474	19.999
SSCN_2	12.580	13.703	16.462	19.934
ASCN_1	12.617	13.721	16.515	20.067
ASCN_2	12.606	13.728	16.508	20.027
MSCN	12.631	13.747	16.548	20.115
HSCN	12.626	13.744	16.546	20.116

TABLE II
Percentage Normalized Propagation Errors

	TE^y_{01}	TE^y_{11}	TE^y_{21}	TE^y_{31}
SSCN_1	+0.357	+0.789	+0.765	+0.732
SSCN_2	+0.774	+0.580	+0.895	+1.129
SSCN(aver.)	+0.565	+0.684	+0.830	+0.930
ASCN_1	-0.132	+0.238	+0.319	+0.320
ASCN_2	+0.138	+0.106	+0.394	+0.562
ASCN(aver.)	+0.002	+0.172	+0.357	+0.441
MSCN	-0.473	-0.253	-0.039	+0.030
HSCN	-0.351	-0.196	-0.017	+0.024

where f and f_0 are the modeled and analytical frequencies and c is speed of light. A summary of these errors is presented in Table II, together with the averaged errors of the results performed by two versions of the ASCN and the SSCN.

It can be seen from Table II that the error pattern for the axial propagation follows the theoretical predictions, that is, the error for TE^y_{01} mode is smallest for the ASCN. To investigate the error distribution for other directions of propagation, we obtain components of the propagation vector in the dielectric [16] and calculate the angle between the propagation vector and the y-axis for each particular mode. We plot, using different symbols, the averaged normalized propagation errors of the ASCN, SSCN and MSCN versus this angle in Fig. 7. In the same figure, we also plot, using dotted lines, the normalized propagation error obtained by solving the dispersion relation (16) for $\varepsilon_r = 2.56$. These errors apply when the waveguide is fully loaded by the dielectric, hence they can be used as an estimate for the maximum error in the problem. On the other hand, an estimated error for the air-filled waveguide is calculated from (16) and plotted using a broken line. The expected error for each of the nodes should fall in the regions bounded by this broken line (air) and an appropriate dotted line (dielectric). As can be seen from Fig. 7, the averaged errors obtained from the TLM simulations with ASCN, SSCN and MSCN show an excellent agreement with the theoretical estimate.

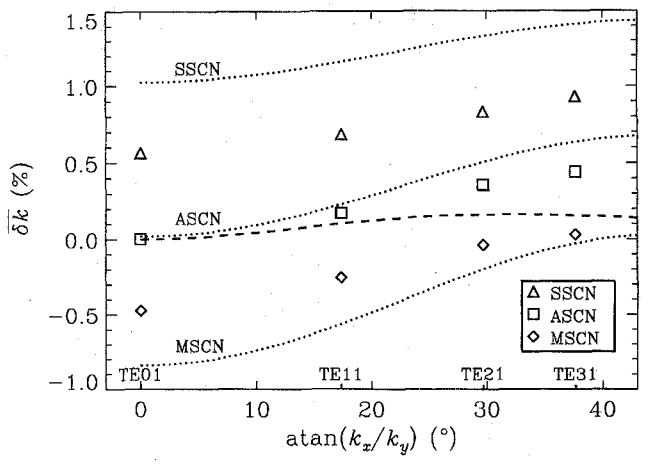

Fig. 7. Comparison of theoretical estimate and numerical results for the propagation error. Dotted lines show theoretical propagation error normalized to $\Delta l/\lambda = 0.1$ in a waveguide fully loaded by dielectric ($\varepsilon_r = 2.56$), while the broken line shows the error for an air-filled waveguide. Symbols show errors obtained by TLM simulations of the partially filled waveguide.

V. Conclusion

Using the framework of the GSCN, we have developed a class of new ASCN's for the TLM method, whose numerical properties can be customized by arbitrary weighting functions. The formulation of the parameters and the dispersion relation of the ASCN offers a powerful practical tool for constructing an optimal nodal configuration by directly investigating dispersion solutions. By exploiting opposite contributions of stubs and link lines to the dispersion, we developed and presented some of the possible weighting functions which minimize propagation errors. The improved accuracy of these schemes was illustrated by the example of modeling an inhomogeneous waveguide. The possibility, opened up by the ASCN, for developing an infinite set of new nodes by simply altering the weighting functions can, no doubt, be further exploited in order to determine other optimal schemes.

References

[1] J. S. Nielsen and W. J. R. Hoefer, "A complete dispersion analysis of the condensed node TLM mesh," *IEEE Trans. Magn.*, vol. 27, no. 5, pp. 3982–3985, Sept. 1991.

[2] M. Celuch-Marcysiak and W. K. Gwarek, "On the effect of bilateral dispersion in inhomogeneous symmetrical condensed node modeling," *IEEE Trans. Microwave Theory Tech.*, vol. 42, no. 6, pp. 1069–1073, June 1994.

[3] V. Trenkic, C. Christopoulos, and T. M. Benson, "Dispersion of TLM condensed nodes in media with arbitrary electromagnetic properties," in *IEEE Int. Microwave Symp. Dig.*, Orlando, Florida, May 1995, vol. 2, pp. 373–376.

[4] ——, "Analytical expansion of the dispersion relation for TLM condensed nodes," this issue, pp. 2223–2230.

[5] P. Berini and K. Wu, "A comprehensive study of numerical anisotropy and dispersion in 3-D TLM meshes," *IEEE Trans. Microwave Theory Tech.*, vol. 43, no. 5, pp. 1173–1181, May 1995.

[6] P. B. Johns, "A symmetrical condensed node for the TLM method," *IEEE Trans. Microwave Theory Tech.*, vol. MTT-35, no. 4, pp. 370–377, Apr. 1987.

[7] R. A. Scaramuzza and A. J. Lowery, "Hybrid symmetrical condensed node for TLM method," *Electron. Lett.*, vol. 26, no. 23, pp. 1947–1949, Nov. 1990.

[8] V. Trenkic, C. Christopoulos, and T. M. Benson, "Theory of the symmetrical super-condensed node for the TLM method," *IEEE Trans. Microwave Theory Tech.*, vol. 43, no. 6, pp. 1342–1348, June 1995.

[9] ——, "Advanced node formulations in TLM—The matched symmetrical condensed node (MSCN)," in *Proc. 12th Annu. Rev. of Progress in Appl. Comput. Electromagn.*, NPS, Monterey, Mar. 18–22, 1996, vol. 1, pp. 246–253.

[10] ——, "A unified approach to the derivation of TLM node parameters," in *1st Int. Workshop Transmission Line Matrix (TLM) Modeling Dig.*, Univ. of Victoria, Victoria, B.C., Canada, Aug. 1995, pp. 23–26.

[11] ——, "Development of a general symmetrical condensed node for the TLM method," this issue, pp. 2129–2135.

[12] C. Christopoulos, V. Trenkic, and T. M. Benson, "Propagation in general media using transmission-line modeling," *Radio Sci.*, Special Issue on Computation in Electromagnetics, vol. 31, no. 4, pp. 965–975, 1996.

[13] V. Trenkic, C. Christopoulos, and T. M. Benson, "Dispersion analysis of TLM symmetrical super-condensed node," *Electron. Lett.*, vol. 30, no. 25, pp. 2151–2153, Dec. 1994.

[14] C. Christopoulos, *The Transmission-Line Modeling (TLM) Method.* Piscataway, NJ: IEEE Press, 1995.

[15] V. Trenkic, "Development and characterization of advanced nodes for the TLM method," Ph.D. dissertation, Univ. of Nottingham, U.K., 1995.

[16] C. A. Balanis, *Advanced Engineering Electromagntics.* New York: Wiley, 1989.

Vladica Trenkic (M'96), for a photograph and biography, see this issue, p. 2135.

Christos Christopoulos (M'92), for a photograph and biography, see this issue, p. 2135.

Trevor M. Benson (M'96), for a photograph and biography, see this issue, p. 2135.